Supplementary Information Appendix

Interplay among nucleosomal DNA, histone tails, and corepressor CoREST underlies LSD1-mediated H3 demethylation

Simona Pilotto[a,1], Valentina Speranzini[a,1], Marcello Tortorici[a,2], Dominique Durand[b,c], Alexander Fish[d], Sergio Valente[e], Federico Forneris[a], Antonello Mai[e], Titia K. Sixma[d], Patrice Vachette[b,c], and Andrea Mattevi[a,3]

[a]*Department of Biology and Biotechnology, University of Pavia, via Ferrata 9, 27100 Pavia, Italy*

[b] *Institut de Biologie Intégrative de la Cellule, CEA, CNRS, UPS 11, 91198 Gif-sur-Yvette, France*

[c]*Université Paris-Sud 11, Bâtiment 430, 91405 Orsay, France*

[d]*Division of Biochemistry and Center for Biomedical Genetics, Netherlands Cancer Institute, Plesmanlaan 121, 1066 CX Amsterdam, The Netherlands*

[e]*Department of Drug Chemistry and Technologies, Sapienza University of Rome, P. le A. Moro 5, 00185 Rome, Italy*

[1]*These authors contributed equally to this work*

[2]*Present address: Division of Cancer Therapeutics, The Institute of Cancer Research, Old Brompton Road 123, SW7 3RP London, United Kingdom*

[3]*To whom correspondence should be addressed. E-mail: andrea.mattevi@unipv.it*

This section reports additional information regarding methodologies, experiments and images as support to the main text.

Protein expression and purification

CoREST1 mutants and H3 Lys4Cys-Cys110Ala double mutant were prepared using standard mutagenesis procedures (QuickChange Mutagenesis Kit, Agilent Technologies Milano, Italy), and purified as the wild type proteins. Human LSD1 (residues 123–852), CoREST1 (305-482), and CoREST3 (200-406), were expressed and purified as previously described (1). The LSD1-CoREST complexes were stored in 25 mM KH_2PO_4 pH 7.2, 5% glycerol. The short LSD1 (residues 171-852) and CoREST1 (residues 305-440) variants were co-purified as for the longer proteins except for the storage buffer which was 25 mM HEPES/NaOH pH 7.4, 200 mM NaCl, 2 mM DTT. Recombinant nucleosomes were prepared using *X. laevis* histones expressed in *E. coli* following the Luger protocol (2) and 146 bp DNA 601 positioning sequence as described previously (3). Native mono-nucleosomes were extracted and purified from fresh chicken blood according to published protocols (4) and stored in buffer 20 mM TRIS/HCl pH 7.5, 1 mM EDTA, and 1 mM DTT.

Procedure for the synthesis of 1-methyl-1-(prop-2-ynyl)aziridinium chloride

Chemistry. Melting points were determined on a Buchi 530 apparatus and are uncorrected. ^{1}H NMR and ^{13}C NMR spectra were recorded at 400 MHz on a Bruker AC 400 spectrometer. Chemical shifts are reported in δ (ppm) units relative to the internal reference tetramethylsilane (Me4Si). EIMS spectra were recorded with a Fisons Trio

1000 spectrometer; only molecular ions (M+) and base peaks are given. All compounds were routinely checked by TLC and ^{1}H NMR. TLC was performed on aluminum-backed silica gel plates (Merck DC, Alufolien Kieselgel 60 F254) with spots visualized by UV light. All solvents were reagent grade and, when necessary, were purified and dried by standard methods. Concentration of solutions after reactions and extractions involved the use of a rotary evaporator operating at reduced pressure of ca. 20 Torr. Organic solutions were dried over anhydrous sodium sulphate. Analytical results are within ± 0.40% of the theoretical values. All chemicals were purchased from Aldrich Chimica, Milan (Italy), or from Alfa Aesar, Milan (Italy), and were of the highest purity.

Reaction. 2-(methyl(prop-2-ynyl)amino)ethanol (1.77 mmol, 0.2 g), previously prepared according to the literature (5), and thionyl chloride (5 ml) were stirred at 80°C for 1 hour. Then the reaction was cooled down to room temperature, the precipitated solid was filtered, washed with diethyl ether (3 x 5 ml) and dried to obtain the pure salt. Melting point: 142-145°C. Yield: 74%; ^{1}H-NMR (DMSO-d6) δ 2.81 (s, 3H, -NCH_3), 3.45-3.49 (t, 2H, -NCH_2CH_2), 3.87 (s, 1H, -CCH), 4.00-4.04 (t, 2H, -NCH_2CH_2), 4.13 (s, 2H, $HCCCH_2$-) ppm; ^{13}C NMR (DMSO-d6) δ 48.5 (2C), 53.9, 58.3, 71.7, 80.8 ppm.

Preparation of semi-synthetic histones

Lyophilized H3 Lys4Cys-Cys110Ala histone was dissolved in 1 M HEPES/NaOH pH 7.8, 4 M guanidinium chloride, 10 mM L-Met, 10 mM DTT. Alkylation was performed in the same buffer using a final 50 mM concentration of the 1-methyl-1-(prop-2-ynyl)aziridinium chloride alkylating agent, as described previously (6). The complete installation of the propargylamine analogue of dimethyl-lysine was confirmed by ESI-

ITMS (LCQ*Fleet* Thermo Scientific Ion Trap) mass spectrometry, indicating that 100% H3 molecules were modified (Figure S12).

Fluorescence polarization assays

DNA and histone peptides binding assays were carried out monitoring the change in polarization properties of fluorescent molecules upon binding to LSD1-CoREST or nucleosomes. The labeling fluorophore was 5(6)-carboxytetramethylrhodamine. In order to allow comparative analysis of binding affinities, all experiments were carried out in the same assay buffer, which consisted of 15 mM KH_2PO_4 pH 7.2, 1 mg/ml BSA, 5% glycerol, and 0-100 mM KCl at room temperature. CLARIOstar (BMG Labtech) or PHERAstar FS (BMG Labtech) plate readers were used with 540 nm excitation and 590 nm emission filters. Experiments were performed in triplicates using 384-well microplates (CORNING, UK).

Direct binding of LSD1-CoREST to DNA was assayed using a 5'-carboxytetramethylrhodamine-AGTCGCCAGGAACCAGTGTCA-3' oligonucleotide (Table S1). A second DNA molecule was also employed, containing a G/T mismatch at position 11 (forward strand 5'-carboxytetramethylrhodamine-AGTCGCCAGGGACCAGTGTCA-3'). Protein samples (2 μM final concentration) were incubated with labeled oligonucleotides (1 nM final) followed by serial 1:1 dilutions with the assay buffer supplemented with 1 nM oligonucleotide as to maintain the same oligonucleotide concentrations in all wells. Experiments were repeated using 5 nM and 10 nM fixed ligand concentrations to confirm consistent binding. The plates were incubated for 10 minutes at room temperature before measurements. Binding of histone

H3 N-terminal tail to LSD1-CoREST was assayed using a C-terminally carboxytetramethylrhodamine-labeled histone H3 peptide with sequence ARTdimeKQTARKSTGGKAPRKQLA (Table S2). Direct binding was assayed by preparing protein samples (2 μM final concentration) with labeled peptide (1 nM final concentration) followed by serial 1:1 dilutions. For competitive experiments, each well contained LSD1-CoREST (60 nM final concentration) and labeled peptide (1 nM final). Next, decreasing concentrations (typically in the 0-2 μM range) of the unlabeled competing peptides were added. Binding of H3 peptides to the nucleosome was detected using very similar protocols (Table S3). Direct binding experiments were performed with 0-4 μM nucleosomes and 1 nM tetramethylrhodamine-labeled peptide. Competitive experiments were carried out with 4 nM nucleosomes, 1 nM labeled peptide, and 0-10 μM competing peptides. For the sake of comparison, binding was probed using both recombinant and chicken blood nucleosomes. Experiments were then repeated using 5 nM and 10 nM fixed ligand concentrations to confirm consistent binding.

For direct experiments, non-linear regression was used to fit the binding curves using fluorophore concentration as constrain, yielding dissociation constants (K_d) according to the following equation:

$$Y = \mathrm{Af} + (\mathrm{Ab} - \mathrm{Af}) \times \frac{(\mathrm{c} + \mathrm{Kd} + \mathrm{X}) - \sqrt{(-c - X - Kd)^2 - 4cX}}{2\mathrm{c}}$$

which indicated that the total recorded signal (Y) depends on that of bound (Ab) and free (Af) fluorescent ligand, as function of total protein concentration (X) and total ligand concentration (c, 1 nM in our case).

As for competitive assays, the non-linear fitting equation was modified as follows:

$$Y = \mathrm{FPf} + (\mathrm{FPb} - \mathrm{FPf}) \times \frac{\frac{1}{2}\mathrm{X} - \frac{1}{2}\mathrm{Kc} - \frac{1}{2}c_n + \frac{1}{2}\sqrt{Kc^2 + 2XKc + 2c_nKc + X^2 - 2Xc_n + {c_n}^2}}{Kd + \frac{1}{2}\mathrm{X} - \frac{1}{2}\mathrm{Kc} - \frac{1}{2}c_n + \frac{1}{2}\sqrt{Kc^2 + 2XKc + 2c_nKc + X^2 - 2Xc_n + {c_n}^2}}$$

This modification takes into account ligand depletion by adding to the fitting non-labeled ligand concentration (c_n) to calculate the new dissociation constant (Kc). Graphs were prepared using GraphPad Prism. Tetramethylrhodamine-conjugated peptides were synthesized at the peptide synthesis facility of Netherlands Cancer Institute, The Netherlands. Conjugated oligonucleotides were purchased from Sigma.

Analytical and preparative chromatography of LSD1-CoREST/nucleosome complexes

Analytical size-exclusion chromatography was performed on silica gel columns WTC-030N5 and WTC-030S5 (Wyatt Technology, California, US) equilibrated in 15 mM TRIS/HCl pH 7.3, 0.4 mM EDTA, and 200 mM KCl at room temperature. LSD1-CoREST (in 25 mM KH_2PO_4 pH 7.2, 5% glycerol) were mixed with semi-synthetic nucleosomes (in 20 mM TRIS/HCl pH 7.5, 1 mM EDTA, 1 mM DTT) at different molar ratios and were typically incubated on ice for 2 hours. Protein elution profiles were recorded with detection wavelengths set at 214 nm (peptide bond), 260 nm (DNA), and 280 nm (aromatic protein side chains) using an AKTAmicro purification system (GE Healthcare). Milligram quantities of the covalent complex were purified on Superdex 200 10/300 (three columns connected in series) equilibrated in 15 mM TRIS/HCl pH 7.5, 0.4 mM EDTA, and 200 mM KCl. A mix containing 20 µM semi-synthetic nucleosomes and 30 µM LSD1-CoREST (1:1.5 molar ratio) in their storage buffers was supplemented with 50 mM KCl and let 4 hours on ice. The elution profile was recorded at 260 nm, 280 nm,

and 400 nm (alkyl-FAD absorbance peak) using an AKTApurifier10 (GE Healthcare). The eluted fractions corresponding to the covalent LSD1-CoREST1/nucleosome complex were collected, mixed 1:1 with salt-free buffer, concentrated in Amicon 30 KDa cut-off (Merck Millipore, Germany), and stored on ice for 2-3 weeks (storage buffer 15 mM TRIS/HCl pH 7.5, 0.4 mM EDTA, and 100 mM KCl).

Gel-shift assay

Gel shift assays were performed using non-denaturant gel electrophoresis on 5% TBE (25 mM TRIS/Boric acid pH 8.2, 1 mM EDTA) acrylamide gels, pre-run for 3 hours at 150V in the same buffer. Equal amount (~2 µg) of LSD1-CoREST1 and semi-synthetic nucleosomes were loaded separately on the gel as standards. Each sample was supplemented with 25% glycerol and the run was performed at 150V for 1 hour in fresh 5% TBE buffer. Gel was first stained with ethidium bromide and visualized using a standard UV transilluminator to check DNA content of each sample. The same gel was then rinsed and stained with Coomassie blue solution (0.1 % Brilliant blue R250, 10% Acetic acid, 25% isopropanol).

Insight gained from data on salt composition

In preparation of the SAXS experiments, we evaluated the effect of varying salt concentrations (i.e. ionic strength) on the efficiency of LSD1-CoREST/nucleosome association. Remarkably, moderately increased salt concentrations (up to 200 mM KCl) turned out to facilitate complex assembly (Figure S13). This effect was even more pronounced for mutants hampered in their DNA binding. For instance, the CoREST1

K418E-N419D protein is a very weak DNA binder (Table S1) and nonetheless, in presence of salt, it becomes able to bind to nucleosome as efficiently as wild type. Based on Table S3 data, the salt promotes the detachment of the histone tails from the nucleosome. In this way, the tails may become fully available for binding to LSD1 active site, which is far less influenced by higher salt concentrations (Table S2). It is such a differential sensitivity to ionic strength of tail binding that ultimately favors formation of the complex, which has mechanistic implications as discussed in the main text.

Small-angle X-ray scattering experiments

SAXS measurements were initially performed on a laboratory instrument Nanostar (Bruker) with a Microstar rotating anode generator, a double multilayer focusing optics, scatterless-slits (design Dr. J.S. Pedersen, Aarhus Univ., Danemark), and a Vantec 2000 electronic detector. 30 µl of sample (either LSD1/CoREST1 or nucleosomes) were placed in a quartz capillary thermalized cell inserted into an evacuated sample chamber. Series of 20 minute frames were recorded in various buffer and salt conditions. A 25 mM HEPES/NaOH pH 7.4, 1 mM DTT, NaCl (0-200 mM) buffer was chosen for subsequent measurements. LSD1-CoREST1 was studied also at the SWING beamline at the SOLEIL synchrotron (Saint-Aubin, France), using a CCD-based detector (AVIEX) and X-rays with a wavelength λ = 1.033 Å. 40 µl of LSD1-CoREST1 solution were loaded onto a size exclusion-HPLC column (Agilent BioSEc-3, 4.6x300 mm) online with the SAXS measuring cell. The solution eluting from the column was circulated through the quartz capillary at a flow rate of 150 µl/min, high enough to prevent any detectable radiation damage. The scattering patterns of the purified 1:1 and

2:1 covalent complexes (15 mM TRIS/HCl pH 7.3, 100 mM KCl, and 1 mM DTT) were recorded at the BM29 SAXS beamline of ESRF with λ = 0.992 Å (Grenoble) (7). Aliquots were diluted two- and four-fold and SAXS patterns were recorded for both complexes at three concentrations (1-5 μM).

Primary data reduction was performed using the Bruker developed software, the SWING in-house software Foxtrot, and IspyB (BM29) (8), respectively. All data were processed using the program package PRIMUS (9). The scattering intensity at the origin I(0) and R_g were evaluated using the Guinier approximation (10). P(r) profiles were determined using the indirect Fourier transform method as implemented in the program GNOM (11), yielding the value of the maximum diameter D_{Max} and an alternative estimate of the radius of gyration. The molecular mass of each sample (LSD1-CoREST1, nucleosome, and complexes) was evaluated by comparison of the forward scattering with that of water recorded in the same capillary using the value of 0.001637 cm^{-1} for the theoretical scattering intensity of water. The Porod volume of each particle was estimated using PRIMUS. Calculation of the Porod exponent for each complex scattering pattern yielded values of 3.9 and 3.5 for the 1:1 and 2:1 complexes respectively, showing that the two particles are essentially compact (12). The atomic coordinates of the crystal structure of LSD1-CoREST1 (PDB code 2V1D) were used to calculate the scattering patterns using the program Crysol (13). The structure of the nucleosome (PDB code 1KX5) was used for nucleosome and the positions of the various N-terminal tails were refined against the experimental data using SASREF (14). The few missing residues at the C-terminal end of LSD1 (residues 837-852; see below) and N-terminal end of CoREST1 (residues 305-307) of LSD1-CoREST1 were

positioned as dummy residues using the program Bunch (14). All atom descriptions were then substituted using the program SABBAC (15).

As gathered from the scattering curves, LSD1-CoREST1 solutions display strong inter-molecular interactions at low ionic strength, leading to higher-order oligomers at protein concentrations as low as ≈10 μM. We reasoned that these interactions might be mediated, at least in part, by the unstructured and highly charged termini of our LSD1 (disordered N-terminal amino acids 124-170) and CoREST1 constructs (disordered C-terminal residues 441-482). Therefore, we produced a shorter version of each protein, LSD1 171-852 and CoREST1 305-440. Indeed, at 200 mM NaCl, the solution turned out to be essentially mono-dispersed, exhibiting an excellent agreement between the measured data and the patterns calculated from the corresponding crystal structure (Figure S8, panel B; this construct was however unsuitable for studying complexes because it led to precipitation upon mixing with nucleosomes). SAXS characterization of recombinant nucleosomes indicated significant inter-particle interactions that increase with salt concentration and distort the scattering pattern at concentrations higher than 100 mM NaCl, in agreement with previous reports (16). The excellent match between measured and calculated (from crystal structure) (17) scattering curves nicely demonstrated that the nucleosomal particles were perfectly reconstituted (Figure S8).

The opposing behavior of the two interacting partners in their response to salt made SAXS characterization of the LSD1-CoREST1/nucleosome clearly challenging. We came to the conclusion that 100 mM NaCl would represent an acceptable compromise to perform such experiments, having also observed that the LSD1-CoREST1/nucleosome complex stably forms at this salt concentration (Figure S13).

Noticeably, a range of 50-150 mM NaCl is typically referred to as “nearly physiological” ionic strengths in nucleosome biophysics literature (18, 19).

References

1. Forneris F, Binda C, Adamo A, Battaglioli E, and Mattevi A (2007) Structural basis of LSD1-CoREST selectivity in histone H3 recognition. *J Biol Chem* 282(28):20070-20074.
2. Luger K, Rechsteiner TJ, Flaus AJ, Waye MM, and Richmond TJ (1997) Characterization of nucleosome core particles containing histone proteins made in bacteria. *J Mol Biol* 272(3):301-311.
3. Lowary PT and Widom J (1998) New DNA sequence rules for high affinity binding to histone octamer and sequence-directed nucleosome positioning. *J Mol Biol* 276(1):19-42.
4. Villa F*, et al.* (2009) Crystal structure of the catalytic domain of Haspin, an atypical kinase implicated in chromatin organization. *Proc Natl Acad Sci U S A* 106(48):20204-20209.
5. Nieman JA*, et al.* (2010) Modifications of C-2 on the pyrroloquinoline template aimed at the development of potent herpesvirus antivirals with improved aqueous solubility. *Bioorg Med Chem Lett* 20(10):3039-3042.
6. Simon MD*, et al.* (2007) The site-specific installation of methyl-lysine analogs into recombinant histones. *Cell* 128(5):1003-1012.
7. Pernot P*, et al.* (2013) Upgraded ESRF BM29 beamline for SAXS on macromolecules in solution. *J Synchrotron Radiat* 20(Pt 4):660-664.
8. Delageniere S*, et al.* (2011) ISPyB: an information management system for synchrotron macromolecular crystallography. *Bioinformatics* 27(22):3186-3192.
9. Konarev PV, Volkov VV, Sokolova AV, Koch MHJ, and Svergun DI (2003) PRIMUS - a Windows-PC based system for small-angle scattering data analysis. *J Appl Crystallogr* 36:1277-1282.
10. Guinier A (1939) Diffraction of X-rays of very small angles – application to the study of ultramicroscopic phenomenon. *Ann Phys* 12: 161–237.
11. Svergun DI (1992) Determination of the Regularization Parameter in Indirect - Transform Methods Using Perceptual Criteria. *J Appl Cryst* 25:495-503.
12. Rambo RP and Tainer JA (2011) Characterizing flexible and intrinsically unstructured biological macromolecules by SAS using the Porod-Debye law. *Biopolymers* 95(8):559-571.

13. Svergun DI, Barberato C, and Koch MHJ (1995) CRYSOL - a program to evaluate X-ray solution scattering of biological macromolecules from atomic coordinates. *J Appl Crystallogr* 28:768-773.
14. Petoukhov MV and Svergun DI (2005) Global rigid body modelling of macromolecular complexes against small-angle scattering data. *Biophys J*.
15. Maupetit J, Gautier R, and Tuffery P (2006) SABBAC: online Structural Alphabet-based protein BackBone reconstruction from Alpha-Carbon trace. *Nucleic Acids Res* 34(Web Server issue):W147-151.
16. Bertin A, Renouard M, Pedersen JS, Livolant F, and Durand D (2007) H3 and H4 histone tails play a central role in the interactions of recombinant NCPs. *Biophys J* 92(7):2633-2645.
17. Davey CA, Sargent DF, Luger K, Maeder AW, and Richmond TJ (2002) Solvent mediated interactions in the structure of the nucleosome core particle at 1.9 a resolution. *J Mol Biol* 319(5):1097-1113.
18. Mutskov V*, et al.* (1998) Persistent interactions of core histone tails with nucleosomal DNA following acetylation and transcription factor binding. *Mol Cell Biol* 18(11):6293-6304.
19. Sun J, Zhang Q, and Schlick T (2005) Electrostatic mechanism of nucleosomal array folding revealed by computer simulation. *Proc Natl Acad Sci U S A* 102(23):8180-8185.

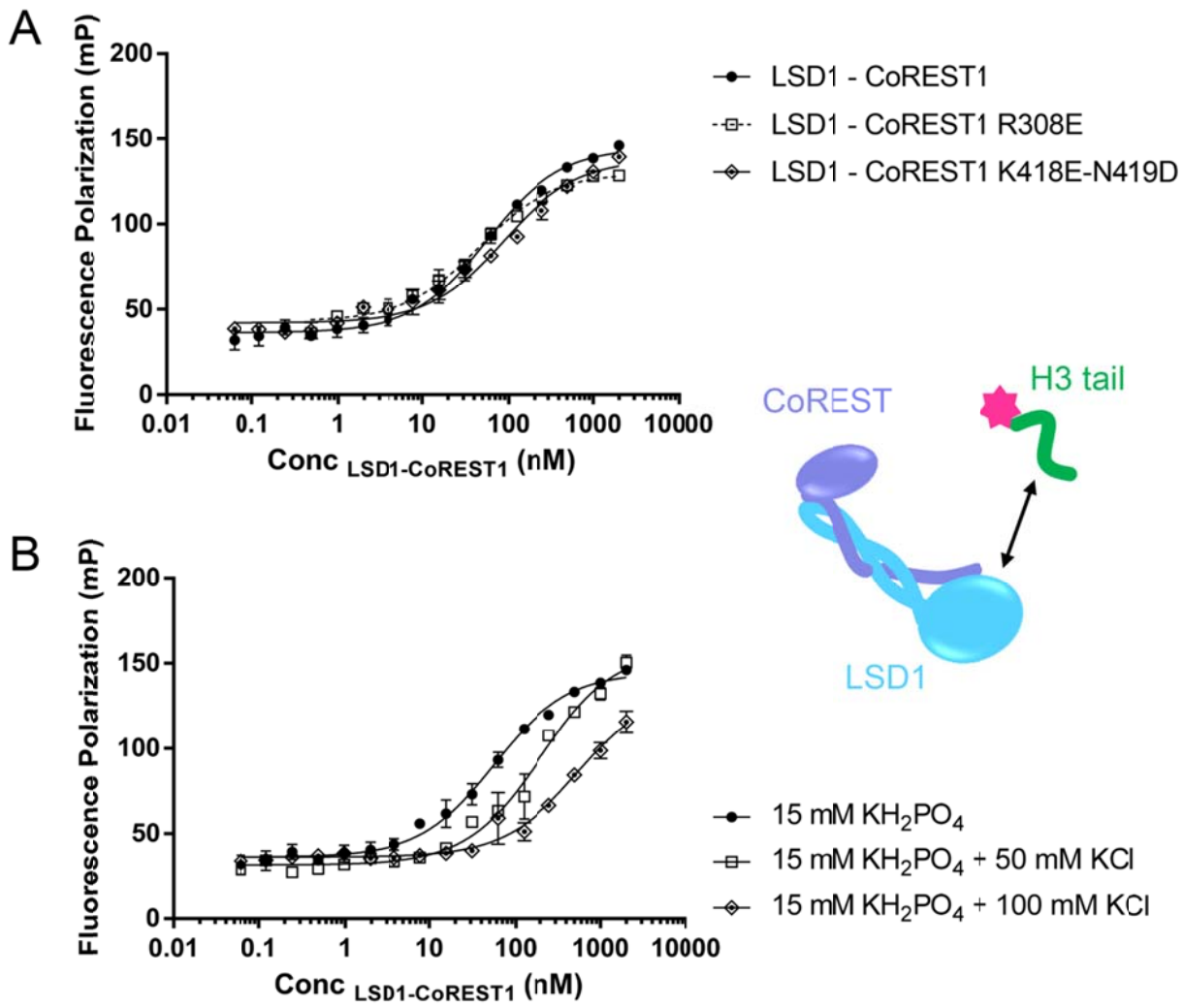

Supplementary Figure S1. Affinities of LSD1-CoREST1 to the H3 N-terminal tail (amino acids 1-21) measured by direct binding. Increasing concentrations of purified LSD1-CoREST1 were incubated with 5(6)-carboxytetramethylrhodamine-conjugated dimethylLys4-H3 peptide (final concentration of 1 nM). Changes were measured in millipolarization (mP) units and plotted against the concentration of LSD1-CoREST1. Error bars correspond to standard deviations for all measurements (n ≥ 3). (A) Binding curves of wild-type and two representative mutants. (B) Effect of buffer ionic strength on binding affinities. The addition of 50 mM KCl to the reaction affects K_d by a factor of ~3.9. Addition of 100 mM salt reduces K_d by a factor of ~10.

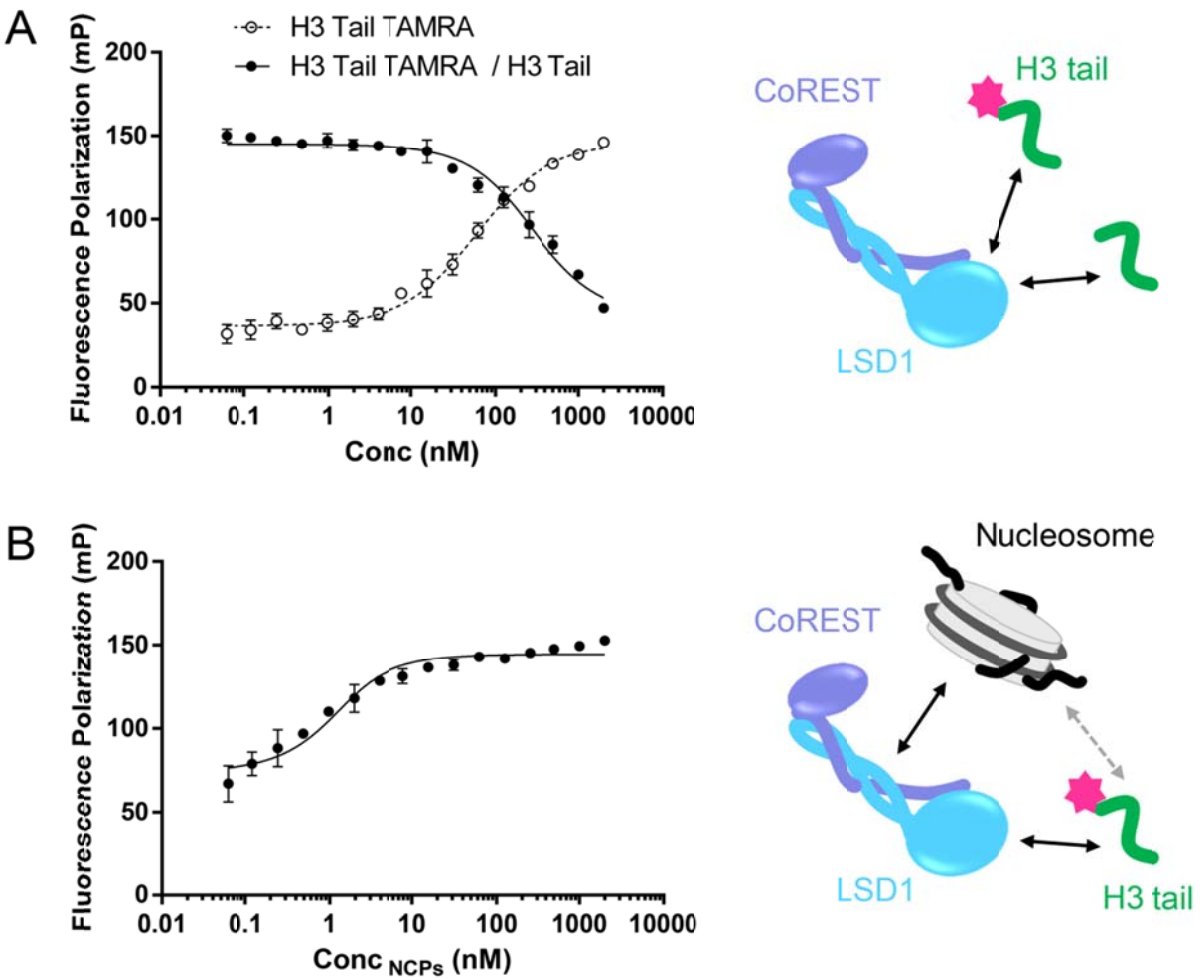

Supplementary Figure S2. Binding of LSD1-CoREST1 to the H3 N-terminal tail measured by competitive assay. (A) Purified LSD1-CoREST1 (final concentration 60 nM) was incubated with carboxytetramethylrhodamine-conjugated H3 peptide (final concentration 1 nM; here named *TAMRA*). Increasing (0-2 μM) concentrations of untagged peptide were then added (here named *H3 Tail*; closed circles). Comparison with the curve and K_d value obtained by direct binding (open circles) demonstrates that the carboxytetramethylrhodamine label does not significantly affect binding affinity. (B) LSD1-CoREST1 (60 nM final concentration) was mixed with tetramethylrhodamine-conjugated H3 peptide (1 nM final). Untagged nucleosomes were then added at increasing concentrations. The curve shows a "binding-like" (instead of a "competition-like" as in panel A, closed circles) trend since the fluorescence polarization increases with nucleosome concentration.

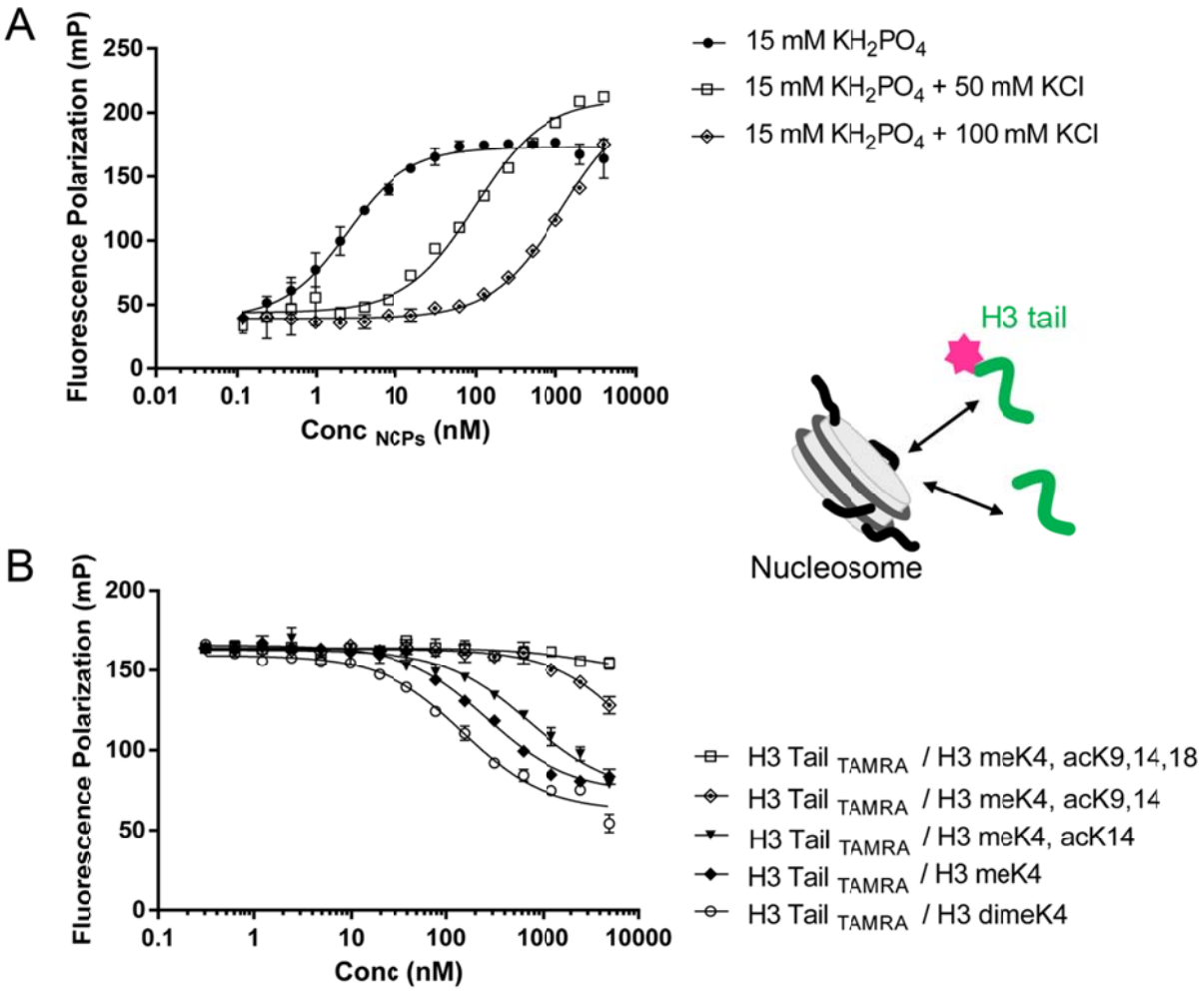

<u>Supplementary Figure S3.</u> Binding of the H3 N-terminal tail to the nucleosomes. (A) Increasing concentrations of chicken-blood nucleosomes (0-4 µM) were incubated with carboxytetramethylrhodamine-conjugated H3 tail peptide (1 nM final concentration). Error bars correspond to standard deviations for all the measurements (n ≥ 3). The addition of 50 mM KCl to the reaction mix reduces affinity by ~ 50-fold, whereas 100 mM KCl causes an even larger (~ 650 times) affinity decrease. (B) Binding affinity of histone tail peptides carrying different modifications on Lys residues were measured by competitive assays. Nucleosomes (final 4 nM) were mixed to 1 nM (final) tetramethylrhodamine-conjugated H3 peptide (dimethylated on Lys4). Untagged H3 peptides with varying Lys acetylations were then incubated at 0-5 µM concentrations.

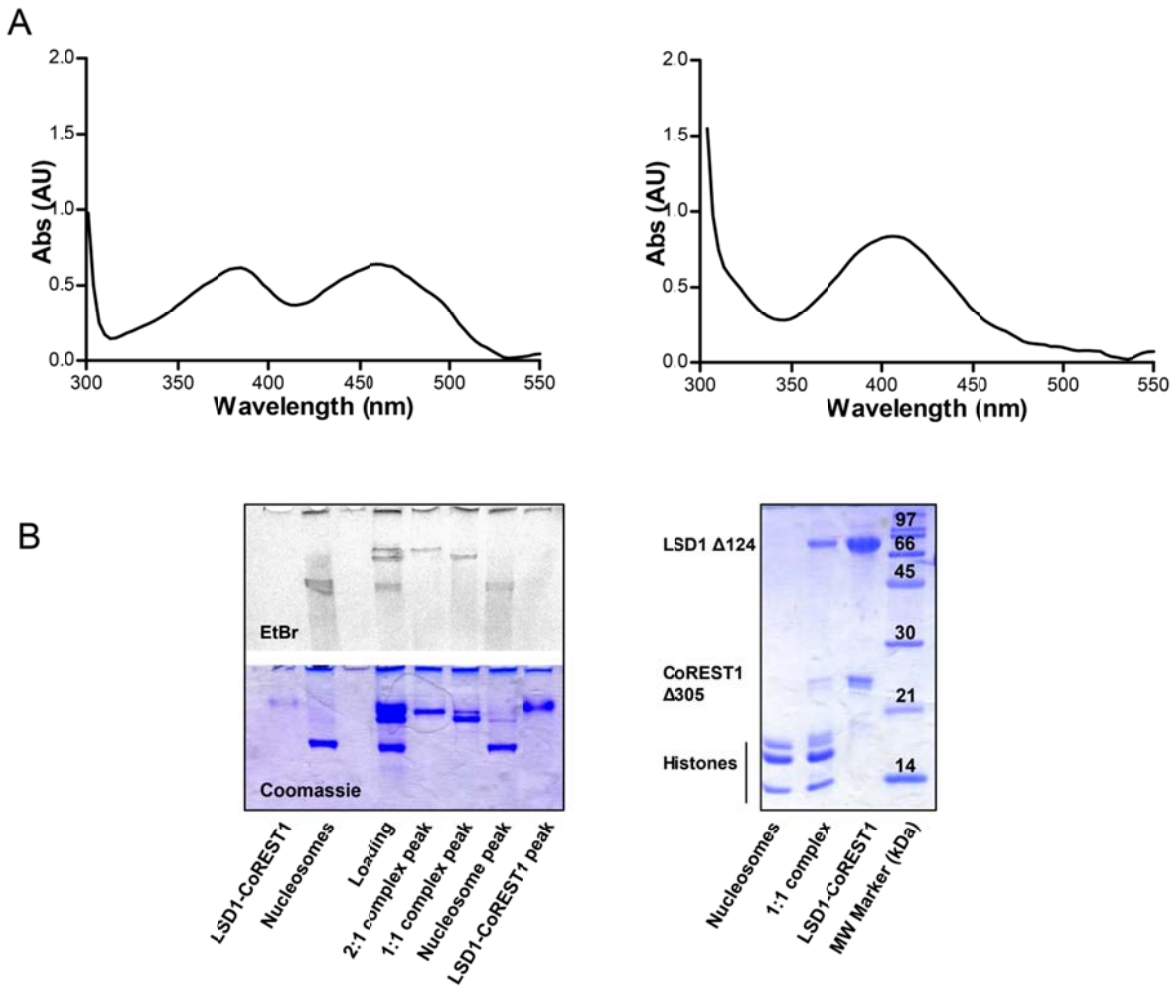

Supplementary Figure S4. Characterization of purified LSD1-CoREST1/nucleosome covalent complexes. (A) Native LSD1-CoREST1 (60 μM) shows the typical absorbance peaks at 380 nm and 458 nm of the oxidized FAD (left). Binding of propargyl-modified histone to FAD causes a spectral change with the formation of a single peak at 400 nm (right). The spectrum was measured on purified 1:1 complex obtained from the experiment shown in Figure 2 of the main text. (B) Electrophoretic analysis of eluted fractions. Left panel shows a gel-shift assay in non-denaturing conditions. Single proteins were loaded as reference in the first two lanes, along with their mixture (Loading) and with samples from each peak eluted from the gel filtration. Compared with the loading, the four species show a different electrophoretic signature. Gel was stained with ethidium bromide to visualize DNA-containing samples and to monitor the different mobility of the species. As expected, the LSD1-CoREST1 sample did not contain DNA. Secondly, coomassie stain allowed the visualization of protein content for each sample. Right panel shows the analysis of the same samples in denaturing conditions (SDS-PAGE) to confirm the identity of the different fractions.

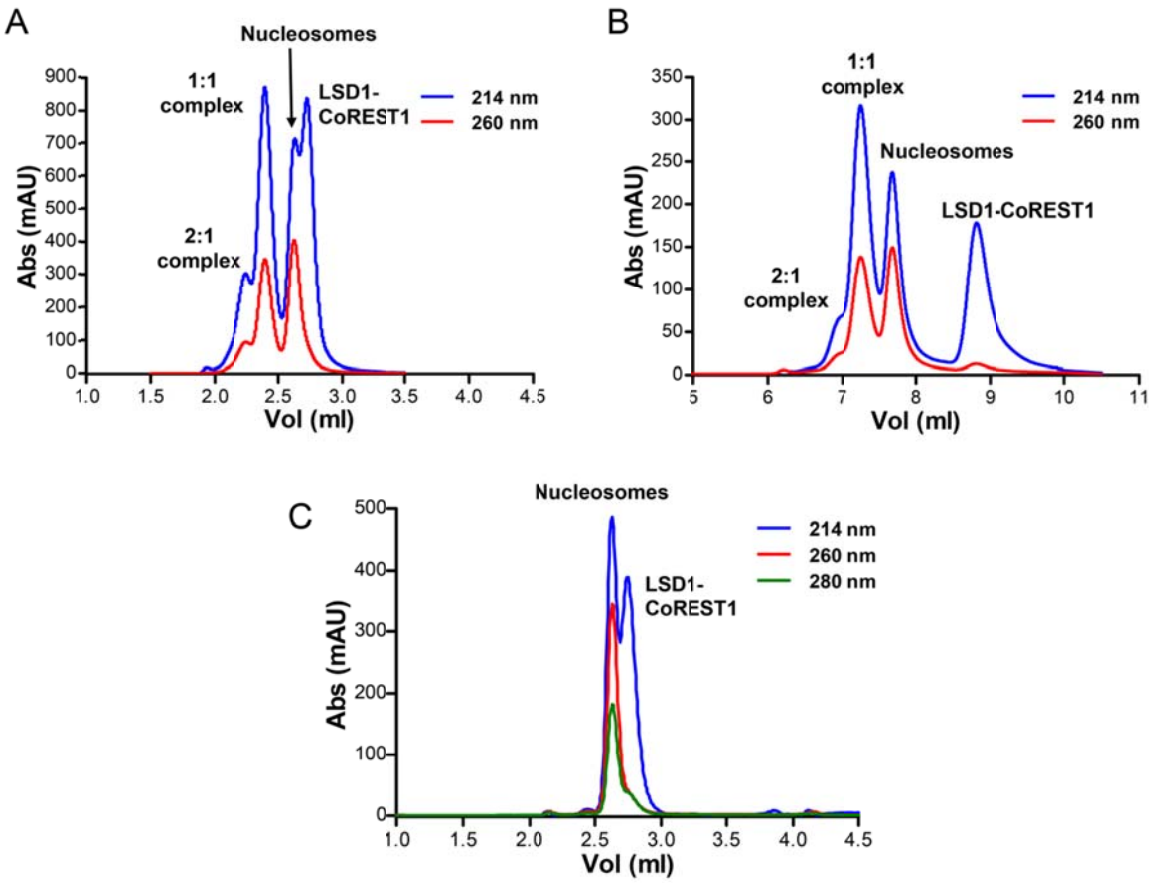

<u>Supplementary Figure S5.</u> Analytical size exclusion chromatography of LSD1-CoREST1/nucleosome complexes. Elution profile of LSD1-CoREST1/nucleosome covalent complexes on Wyatt 030N5 (4.6 x 300 mm; A) and 030S5 (7.8 x 300 mm; B) silica columns. Both columns separate four species. (C) Native recombinant nucleosomes mixed with LSD1-CoREST1 (1:1.5 molar ratio) dissociate and do not co-purify in gel filtration (Wyatt 030N5 as in panel A). The elution volumes are identical to those observed for free nucleosomes and LSD1-CoREST1 as it can be gathered from comparison with the third and fourth peaks of the experiment in panel A. Absorbance at 214 nm and 280 nm monitors protein (peptide bond) and 260 nm monitors DNA.

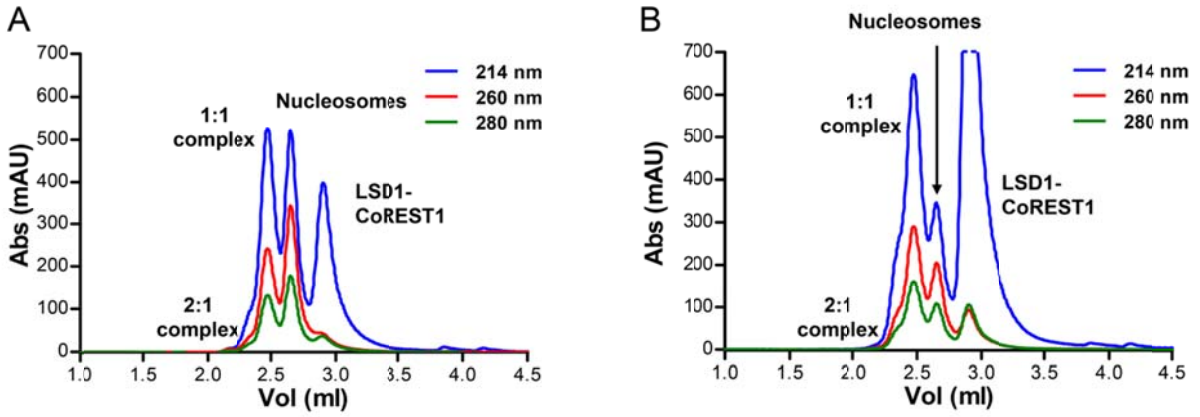

<u>Supplementary Figure S6.</u> Comparison between elution profiles of different LSD1-CoREST1/nucleosome mixtures. LSD1-CoREST1 and semi-synthetic nucleosomes were mixed at (A) 1.5:1 or (B) 4:1 molar ratio for two hours. Increased amounts of LSD1-CoREST1 favor complex formation and decrease free nucleosomes, which, however, remain present in all experiments.

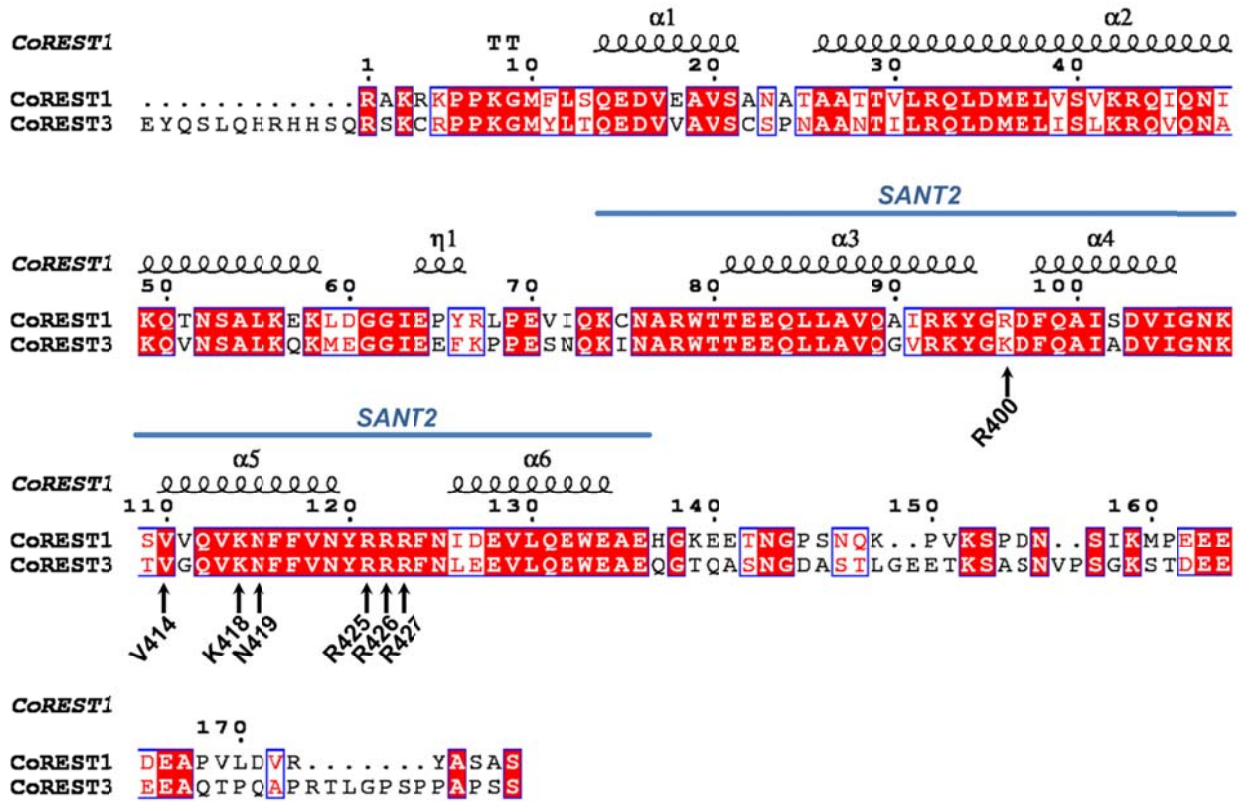

Supplementary Figure S7. Comparison of CoREST1 and CoREST3 protein sequences. Sequence alignment of the human CoREST1 (residues 305-482, Uniprot accession Q9UKL0) and CoREST3 (residues 200-401, Uniprot accession Q9P2K3). Secondary structures elements and sequence similarities representations were computed with ESPript (http://espript.ibcp.fr) using as a PDB input 2V1D (chain B, corresponding to CoREST1). Blue boxes frame conserved blocks, in which red-background residues represent the highest conservation. Black arrows point out the residues affecting DNA binding, all belonging to SANT2 domain (as underlined in blue). Top numbering refers to CoREST1, for which residue 1 corresponds to Arg305. CoREST1 and CoREST3 have identical three-dimensional structures but differ for 69 amino acid changes (not considering insertions in CoREST3), 9 of them located in the SANT2 domain whose cumulative effect may account for the different binding properties (Table S1).

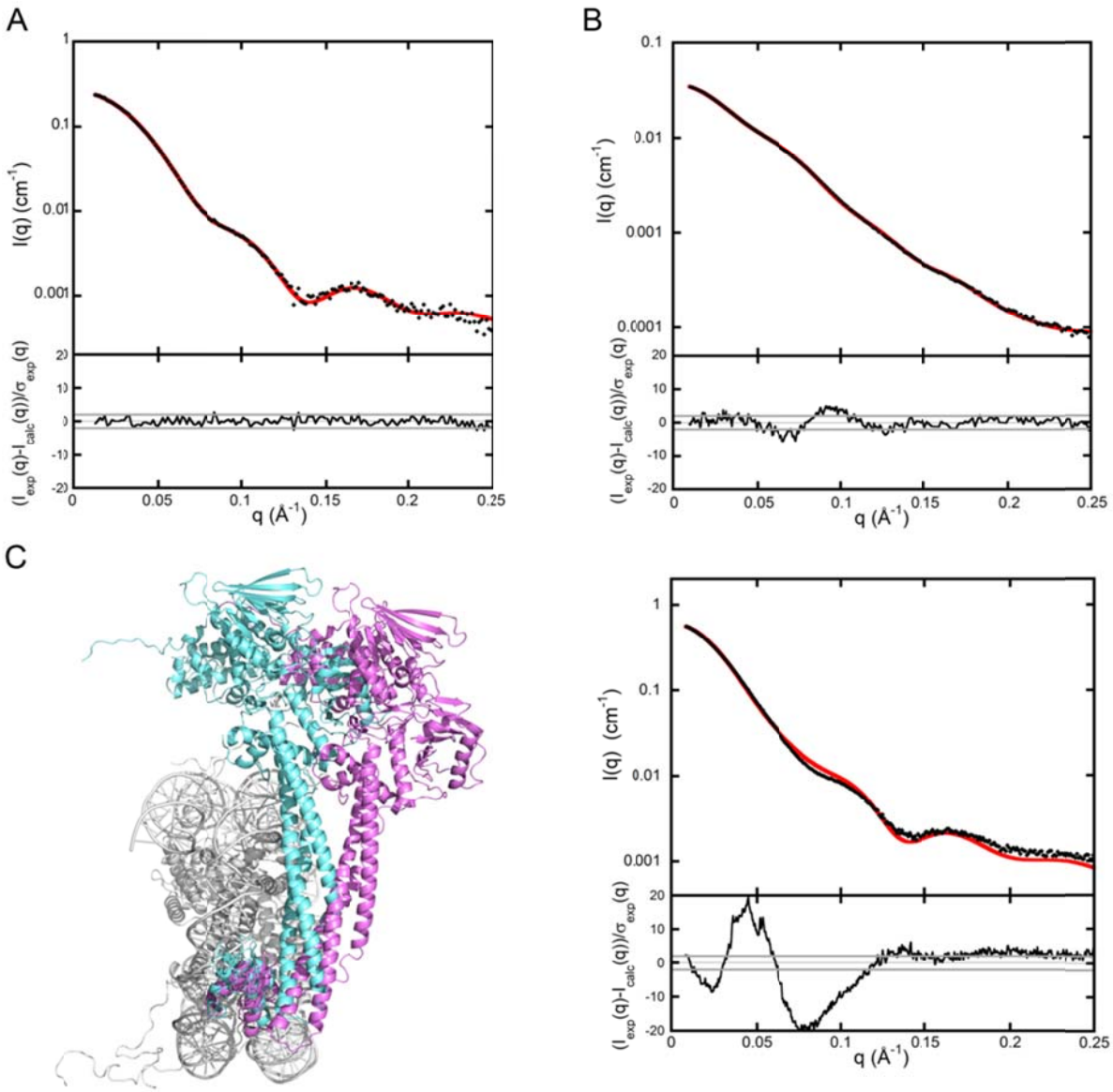

Figure S8. **SAXS experiments.** (A,B) SAXS patterns of isolated LSD1-CoREST1 and nucleosome. Experimental scattering curves (black dots) for recombinant nucleosomes (A) and recombinant LSD1-CoREST1 (B; construct 170-852 for LSD1, 305-440 for CoREST1, Table S4). Data are reported as the intensities I(q) on a logarithmic scale *vs* the momentum transfer q. The curves calculated from the respective three-dimensional structures (PDB entries 1KX5 for nucleosomes and 2IW5 for LSD1-CoREST1) are shown in red. Residuals of each fitting are presented at the bottom.(C) Sensitivity of the SAXS pattern to the mutual arrangement of LSD1/CoREST1 and nucleosome. LSD1/CoREST1 in the best fitting position (cyan; Figure 5) was rotated by *ca* 20° with respect to the mid-plane of the nucleosome (magenta). The calculated SAXS pattern of the rotated model (in red) is shown together with the experimental curve (in black) of the covalent 1:1 complex (right panel). The bottom graph reports the reduced residuals that display large amplitude oscillations (χ^2-value = 7.8).

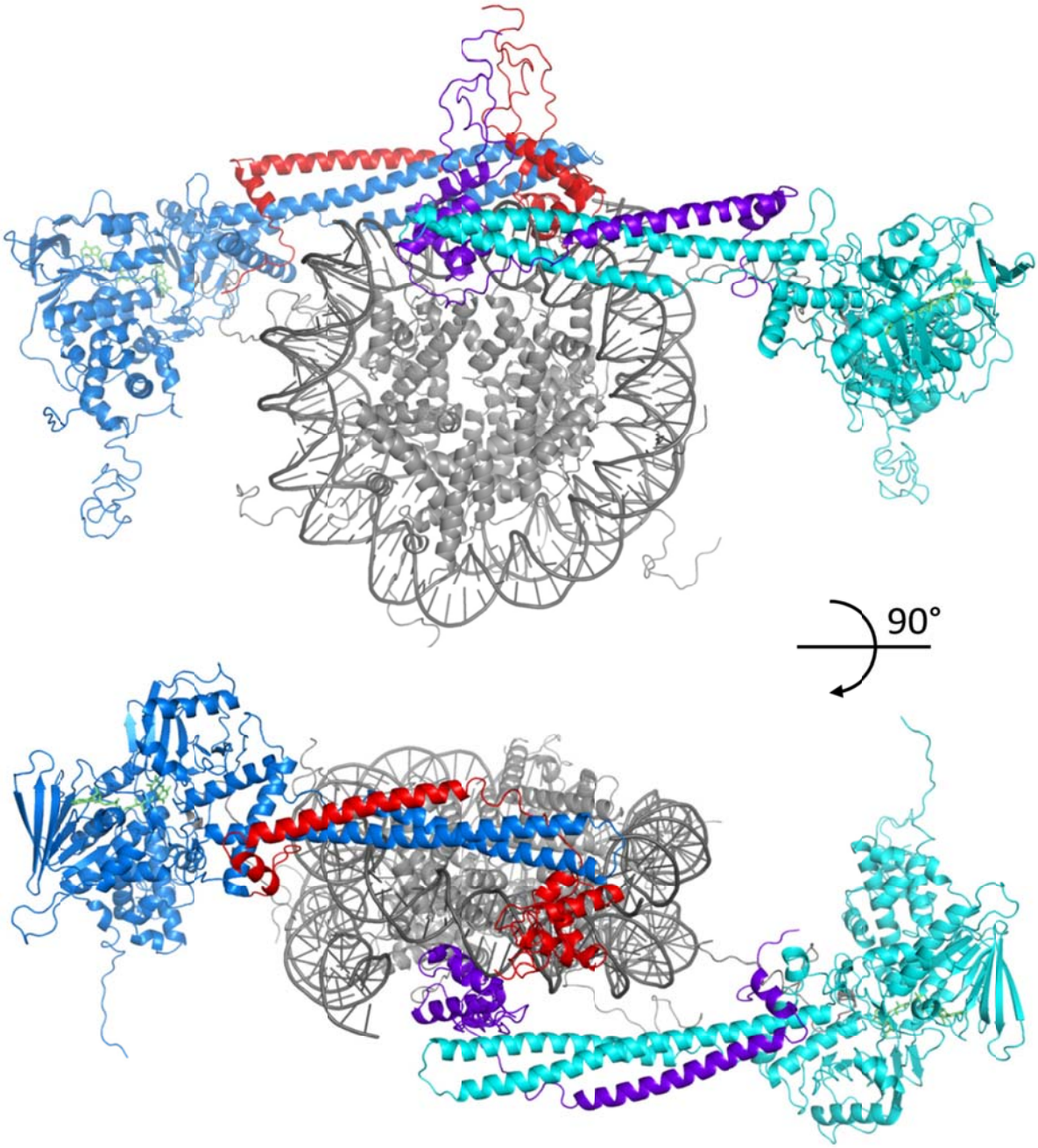

<u>Supplementary Figure S9.</u> Orthogonal views of the model for LSD1-CoREST1/nucleosome 2:1 complex. Symmetric 2:1 complex fitting the SAXS experimental data shown in Figure 5B.

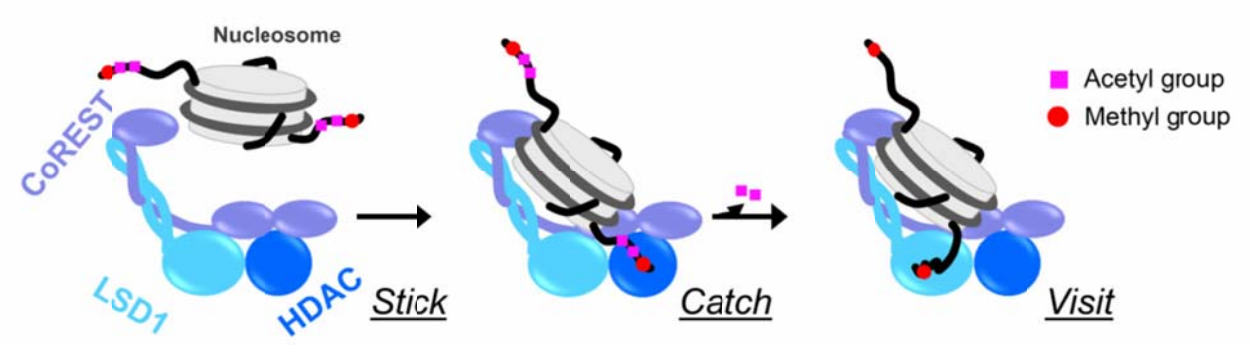

Supplementary Figure S10. Working model for the LSD1-CoREST-HDAC multienzyme complex. Association to DNA by CoREST enables the detached (or weakly retained) hyperacetylated H3 tail to be caught by the HDAC active site. After deacetylation, the tail can visit the LSD1 active site rather than fold back to the nucleosome, whose DNA is occupied by CoREST.

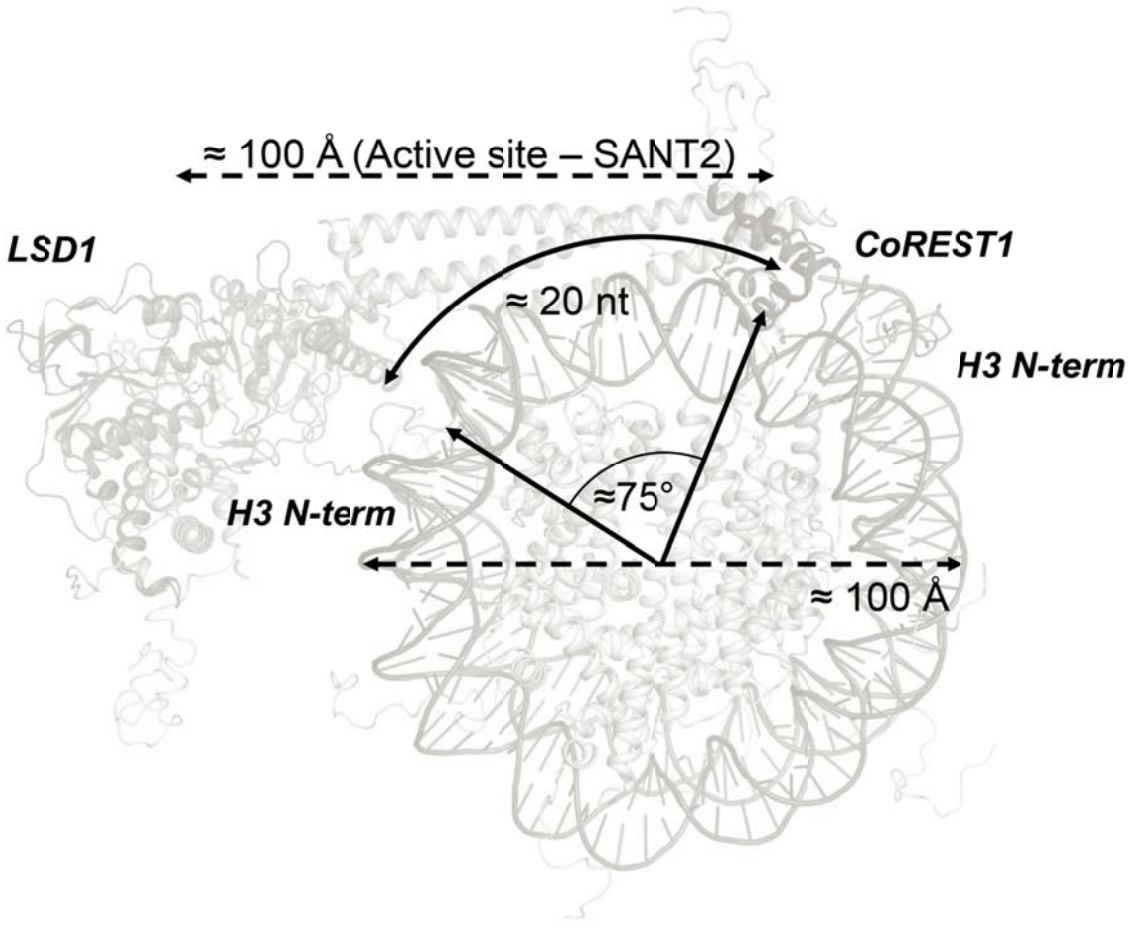

Supplementary Figure S11. Geometric features of the structural model for nucleosome recognition by LSD1-CoREST1. The demethylase clamps the nucleosome in such a way that the SANT2/DNA contact point and the H3 tail bound to the LSD1 active site are separated by approximately 20 base pairs of nucleosomal DNA.

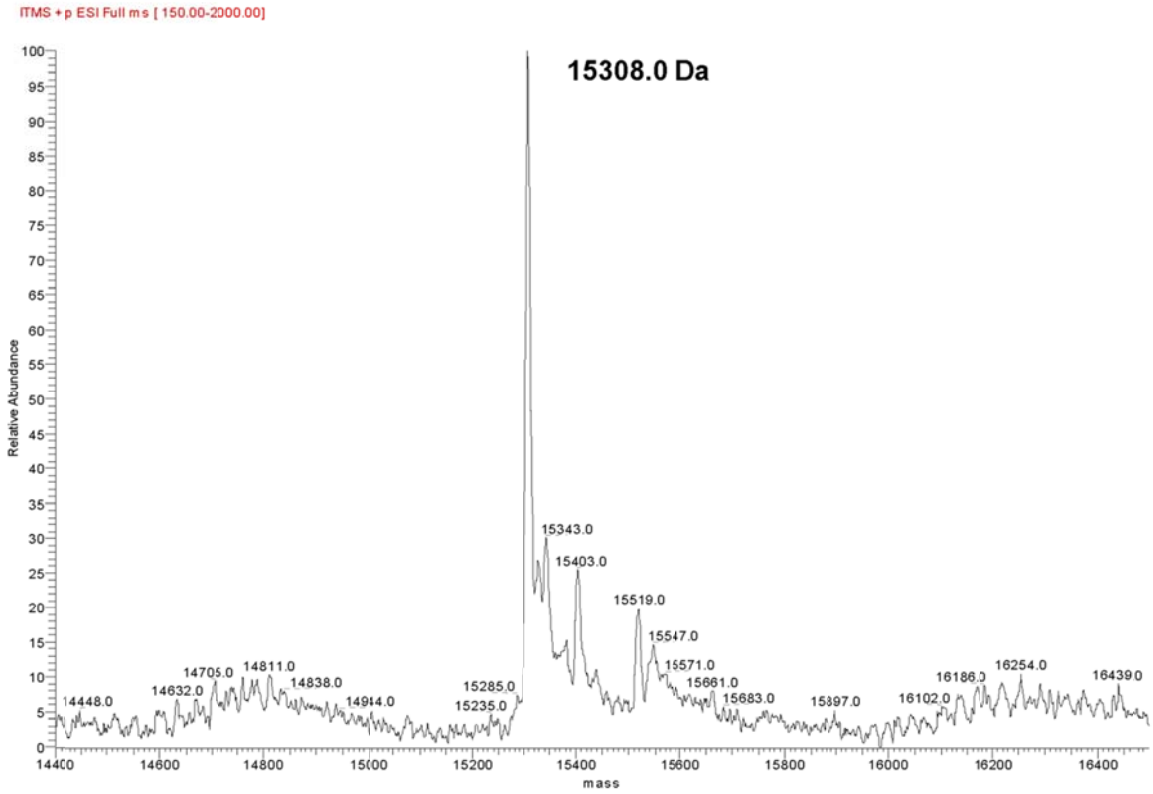

<u>Supplementary Figure S12</u>. Mass spectrum on H3 propargyl-Lys4 analogue. The installation of the propargylamine analogue of dimethyl-lysine on the mutated H3 histone (H3 Lys4Cys-Cys110Ala, 15216 Da), was analyzed by ESI-ITMS mass spectrometry. After the reaction, the protein mass increases of 92 Da as confirmed by the analysis (100% relative abundance, 15308 Da).

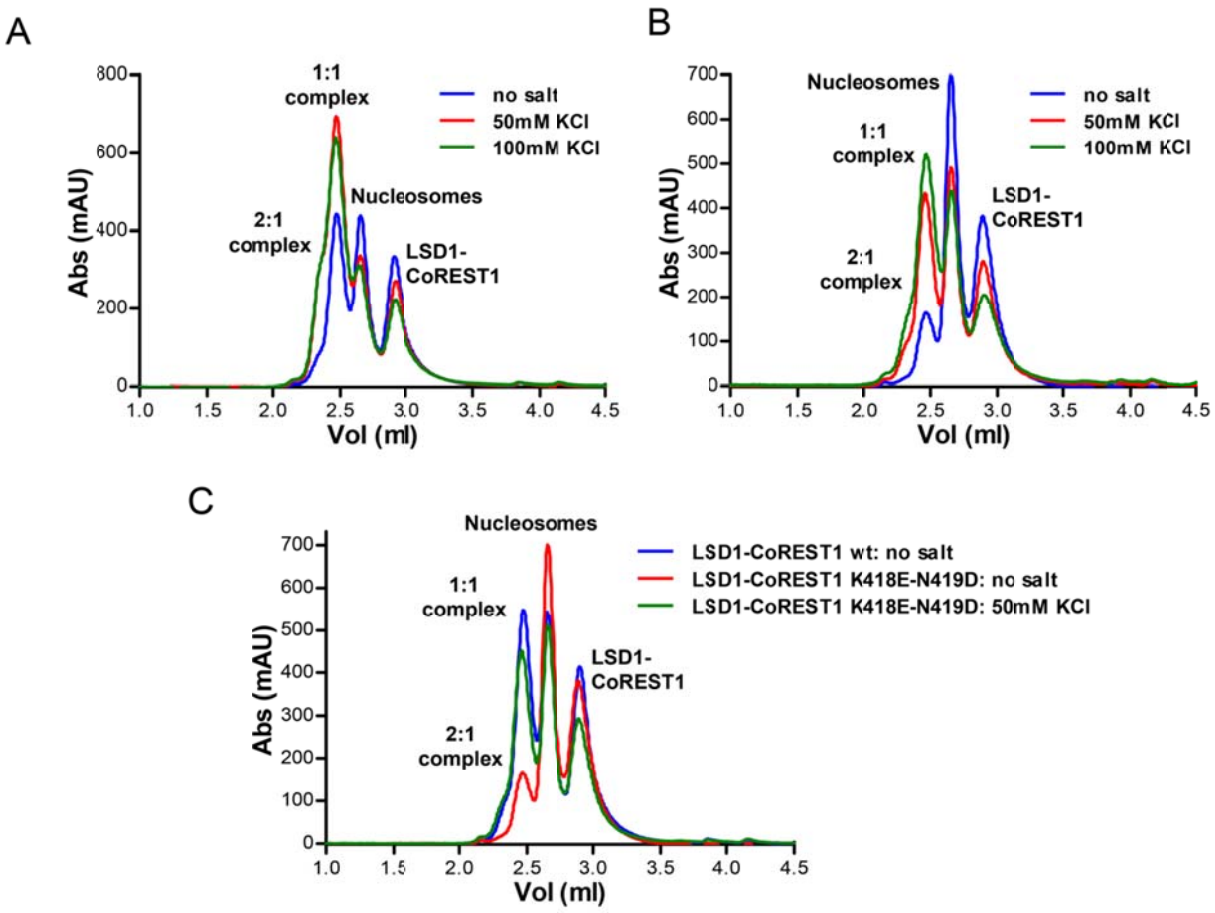

<u>Supplementary Figure S13.</u> Elution profiles of LSD1-CoREST1/nucleosome mixtures incubated at increasing salt concentrations. LSD1-CoREST1 and semi-synthetic nucleosomes were mixed at 1.5:1 molar ratio in buffers supplemented with 0-100 mM KCl. (A) LSD1-CoREST1 wild type. (B) LSD1-CoREST1 K418E-N419D. (C) Comparison of elution profiles in A and B. In the case of CoREST1 mutant, the addition of 50 mM KCl improves complex formation which is at the same level as that for the wild type protein assayed in the absence of salt.

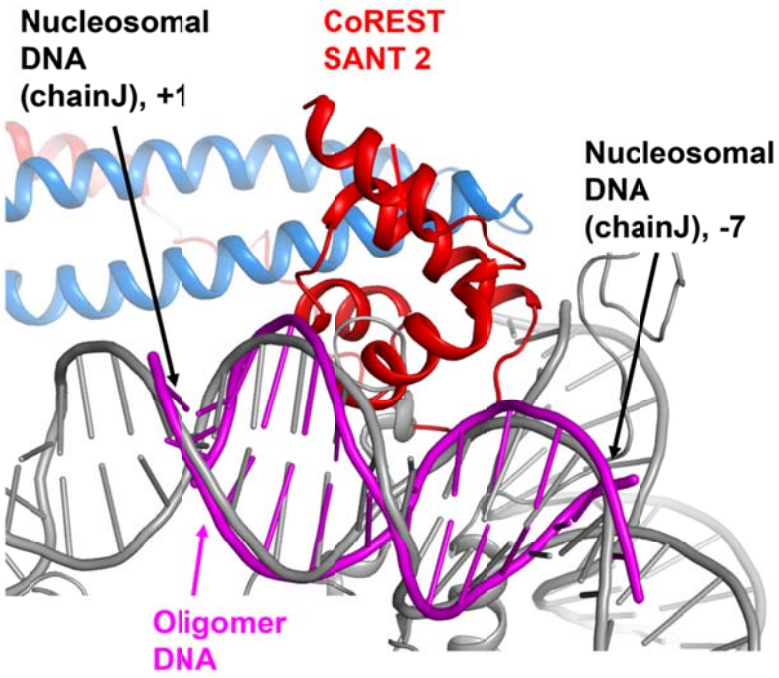

<u>Supplementary Figure S14.</u> Detail for three-dimensional model generation of LSD1-CoREST1/DNA. Close-up view of the superposition of LSD1-CoREST1/DNA model shown in Figure 3 of the main text onto the nucleotides (-J7)-(+J1) of nucleosomal DNA structure (PDB: 1KX5).

Supplementary Table S1

Binding of LSD1-CoREST to DNA	
	K_d (nM)*
LSD1-CoREST 1	72.2 ± 5.3
	103.5 ± 7.3†
LSD1-CoREST 1+ 25 mM KCl	176.1 ± 40.7
LSD1-CoREST 1+ 50 mM KCl	~ 2000
LSD1-CoREST 1+ 100 mM KCl	> 2000
LSD1-CoREST3	405.4 ± 26.5
LSD1-CoREST1 R308E	44.7 ± 4.1
LSD1-CoREST1 K312E	103.9 ± 13.5
LSD1-CoREST1 P369E	38.7 ± 4.1
LSD1-CoREST1 C379D	129.8 ± 12.0
LSD1-CoREST1 A381E	86.5 ± 17.0
LSD1-CoREST1 R400E	529.5 ± 62.5
LSD1-CoREST1 V414E	497.3 ± 68.5
LSD1-CoREST1 K418E	739 ± 84.6
LSD1-CoREST1 N419D	481 ± 152.5
LSD1-CoREST1 K418E-N419D	> 2000
LSD1-CoREST1 R425E	498 ± 155.2
LSD1-CoREST1 R426E-R427A	101.4 ± 15.4

* All K_d values were measured using double stranded DNA with the sequence 5'-carboxytetramethylrhodamine-AGTCGCCAGGAACCAGTGTCA-3'.
† Experiment carried out using DNA sequence 5'-AGTCGCCAGGGACCAGTGTCA-3' which contains a G instead of A at position 11 (underlined).

Supplementary Table S2

Binding of the H3 N-terminal peptide to LSD1-CoREST			
	K_d (nM)		
LSD1-CoREST 1	55.8	±	5.1*
	114.6	±	19.4†
LSD1-CoREST 1 + 50 mM KCl	197.9	±	21.9*
LSD1-CoREST 1 + 100 mM KCl	528.3	±	102.2*
LSD1-CoREST 1 R308E	44.7	±	4.1*
LSD1-CoREST 1 K312E	103.8	±	7.1*
LSD1-CoREST 1 K418E-N419D	87.1	±	11.7*

* K_d was measured by direct binding assay using a 21-amino acid peptide corresponding to the H3 N-terminal tail (ARTdimeKQTARKSTGGKAPRKQLA-carboxytetramethylrhodamine).
† Measured by competitive assay.

Supplementary Table S3

Binding of H3 peptides to the nucleosome*

Peptide	K_d (nM)
dimethylLys4, acetylLys9, acetylLys14, acetylLys18	> 5000
dimethylLys4, acetylLys9, acetylLys14	> 5000
dimethylLys4, acetylLys9	319.5 ± 0.2
dimethylLys4	6.9 ± 0.2
dimethylLys4	1.9 ± 0.3†
dimethylLys4	2.2 ± 0.5†,‡
dimethylLys4 + 50 mM KCl	98.3 ± 12.1†
dimethylLys4 + 100 mM KCl	1174 ± 94.7†
monomethylLys4	15.5 ± 0.2

* K_d values were measured with modified ARTKQTARKSTGGKAPRKQLA peptides using a competition assay with ARTdimeKQTARKSTGGKAPRKQLA-carboxytetramethylrhodamine. The data listed in the table were measured with nucleosomes purified from chicken erythrocytes.
† Measured by direct binding assay.
‡ Measured using recombinant nucleosomes.

Supplementary Table S4

	Structural parameters derived from SAXS analysis *			
	R_g (Å) Guinier	R_g (Å) P(r)	D_{Max} (Å)	Vol_{Porod} (Å^3)
Nucleosome	42.6 ± 0.2	42.6 ± 0.2	140	390,000
LSD1-CoREST1†	44.0 ± 0.5	46.0 ± 0.5	160	130,000
Covalent 1:1 complex‡	55.4 ± 1.0	55.2 ± 1.0	180	570,000
Covalent 2:1 complex‡	65.0 ± 1.0	64.9 ± 1.0	230	715,000

* Calculated with the programs PRIMUS and GNOM.
† Measured with the construct LSD1 171-852/CoREST1 305-440.
‡ Measured with the construct LSD1 123–852/CoREST1 305-482. The construct LSD1 171-852/CoREST1 305-440 was unsuitable for studying complexes because it led to precipitation upon mixing with nucleosomes.